The Wonderful World of High Kubo Number: "Random" Processes and Stochastic Dynamics

Lecture by P.H. Diamond, Summary by R. Masline

May 13, 2019

Contents

1 Introduction

In this section, we will continue our discussion of transport and stochasticity with an investigation of high Kubo number, percolation, and diffusion in system. As we have discussed previously, the Kubo number can be approximated as the ratio of the scattering length to the decorrelation length, or

$$Ku \sim \frac{l_{ac}}{l_c} \sim \frac{\tau_{ac}}{\tau_c}. \tag{1}$$

We recall that diffusion is the method of transport for low Kubo number systems. For low Kubo number, stochasticity comes from the actual particles and their orbits. In contrast, for high Kubo number systems, transport is percolative, and stochasticity in these systems comes from features of the actual media itself. For high Kubo number, the limit is a static random medium of scatterers.

The differences between diffusive and percolative processes can be illustrated by a particle moving in a grid of tiles [1]. In a diffusive process, a particle would have equal probability (each 1/2) of moving to a tile to the left or right, independent of its previous move, as in figure 1(a). The actual "board" of tiles in this system has no bearing on the actual movement of the particle, and the particle has no "memory" of where it has been. In a percolative process, since the motion is defined by the medium itself, each tile would "push" the particle either right or left, moving steadily in one direction, until it reaches successive points in the opposite direction, as in figure 1(b). In the percolative case, history matters; the previous tiles encountered by the particle are the ones that have determined its ultimate position at any given time.

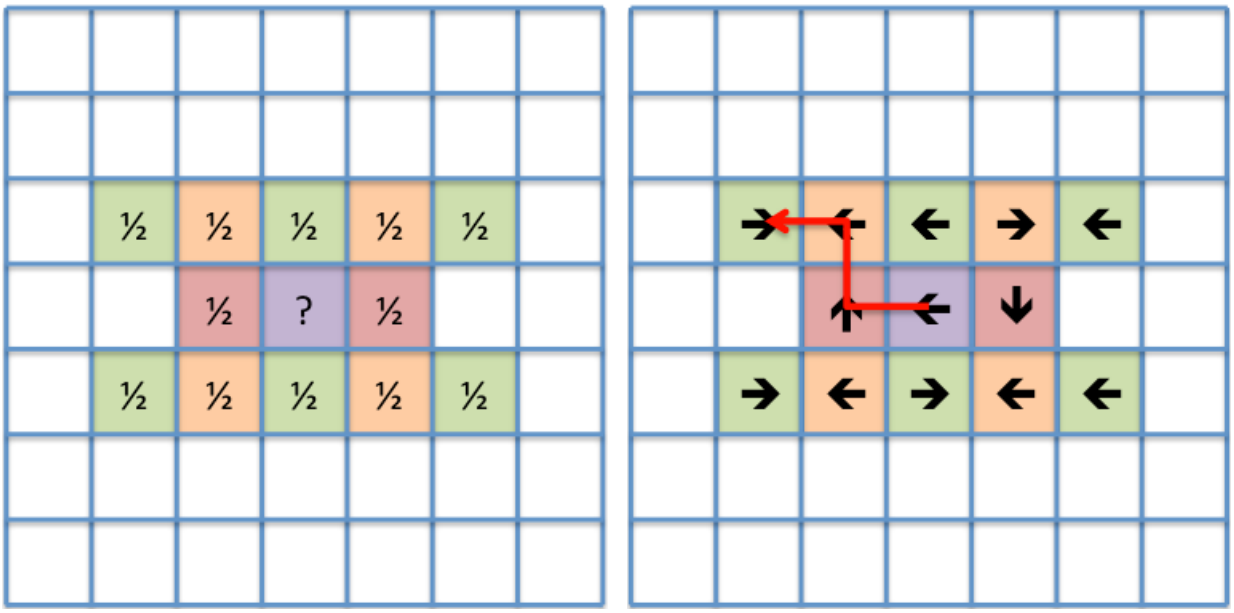

(a) Path of a particle in a diffusive process. Since there is equal probability for each option, the outcome is not dependent on the grid itself.

(b) Path of a particle in a percolative process. The path is set by the grid.

Figure 1: Two “maps” of particle transport on a grid. In each case, the particle starts on the purple tile, moves to a red tile, then an orange tile, and ends on a green tile. The path of the particle depends on whether the system is diffusive (a) or percolative (b).

To emphasize the effect of the topology of the system, as an additional illustrative measure, we can hypothesize an arrangement of magnetic cells, discussed in the previous lecture summary, where the ensemble of cells is a static, disordered medium. Each cell can be treated as a contour, with peaks and valleys and paths along which particles can move. Here, the autocorrelation length corresponds to the paths along which the particle moves through the peaks and valleys in the system. This allows us to find the percolation limit, which can be determined as $l_{ac} \to \infty$, which is defined by the topology of the peaks and valleys in our magnetic cell configuration.

Here, we will discuss some of the fundamental elements of percolation as a physical process and as a model for more complex systems. In Section 2, we will begin by discussing our motivations for studying percolation: the "why?", "what?", and "how?" of our analysis. Then, in Section 3, we will elaborate on these fundamental questions by developing our model of percolation using scaling relations and looking at real examples of percolation problems. We will continue by examining more complex systems involving high Kubo transport and irreversibility in Section 4, and end with concluding remarks in Section 5.

2 Motivation

2.1 Why Percolation?

It is useful to study percolation to give a framework for the discussion of avalanching, which is relevant in the field of plasma physics and many others.

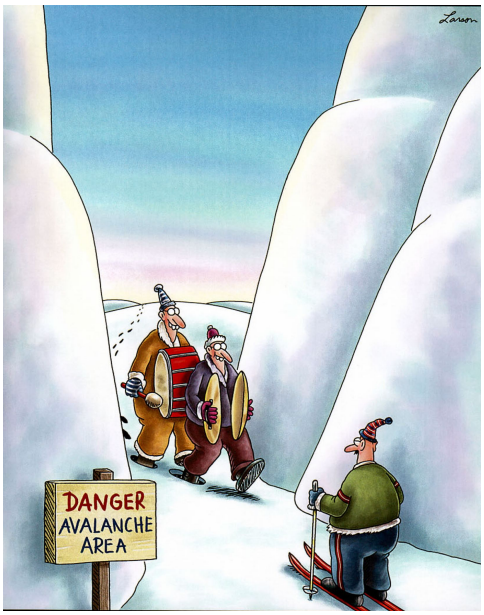

(a) Experimentalists in Physics 235. Taken from [2].

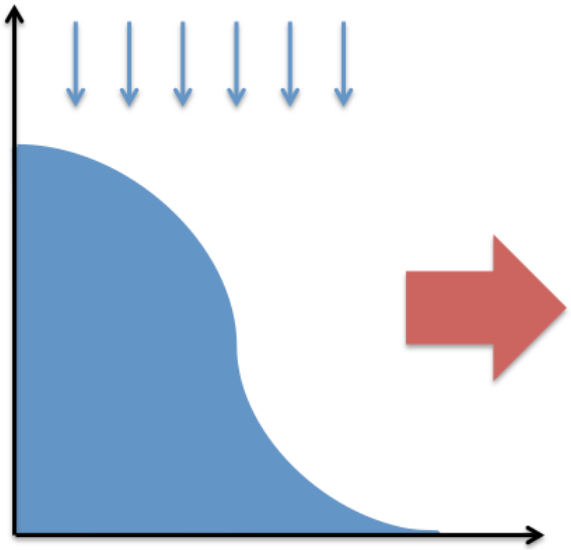

(b) Graphical representation of an avalanche. The blue arrows represent a perturbation, the blue heap represents the system, and the red arrow represents the outward flow when the blue arrows cause the system to reach critical mass.

Figure 2: Two examples of an incoming avalanche.

To provide a brief "spoiler" for the future discussion of avalanching in this course, avalanching is a phenomenon where a few particles cause a group of particles to reach a critical value, and the entire organization of the system changes in one moment (see figure 2). Avalanches are an actual observable phenomenon; they exist in all systems with $\nabla\Gamma$ and in gyrokinetic systems. Perhaps the most familiar colloquial example of an avalanche is a sheet of snow rapidly moving down a hill as a response to some stimulus (whether it be a perturbation in noise, additional snowfall, or an unlucky mountaineer making a tragic misstep).

Without going too much into detail on avalanching at this point in the course, the key takeaway for our discussion and the motivation for this study of percolation is that there is emergent large-scale order from local interactions. In 2D, percolation clusters look like avalanches, with many particles moving at once, which means that we can use the properties of universality and scaling from percolation as a fundamental model for studying avalanching. Thus, an understanding of the ideas and mathematics behind percolation is useful to developing our knowledge of avalanching.

2.2 Basis

One of the first analyses of percolation in random media was presented by Broadbent and Hammersley in the late 1950's [1]. Similarly, Edwin Harold Hurst was interested in similar phenomena in hydrology; in particular, he looked at pressure-driven flow through rocks, such that

$$q = \frac{-k\vec{\nabla}P}{\mu}, \tag{2}$$

where q is the flow and k is the permeability (or resistance) in the medium.

The crucial takeaway from Broadbent and Hammersley's work is that the percolation through a medium is dependent on the probability that a fluid can enter a channel in the system. In the example described in Section 1, the probability for a particle to "enter" onto a new "tile" to progress forward is 1/2. In a more robust example, relevant to Hurst's work and as illustrated in figure 3, a fluid passing through a rock might have several paths through which it could travel. The condition for the fluid to be able to move through any channel is that the channel must be large enough for the fluid to move through it, meaning that there is a probability for each path to be wide enough to allow for passage of the fluid molecule. Essentially, this is a system where there is flow through a random maze of pipettes (that are wide enough for the fluid molecules to fit through). This establishes an important concept in the study of percolation: the innate connection to probability, which allows us to develop analytical tools that are based in statistical analysis.

A key difference in these two examples of single-particle and fluid percolation is the idea of bulk motion - many particles acting together as a "cluster". This introduces additional complexity to our analysis, as we are now dealing with both sets of particles and corresponding "end gaps" between percolation clusters. It makes sense, then, to look at particles in terms of distributions and corresponding probabilities, describing the system by the statistical distributions of the probability that a particle will (or will not) exist in that location at the snapshot of the percolation. As such, percolation cluster distribution functions (which will be discussed in Section 3) like $n_s(p)$ and $sn_s(p)$ are measures of emergent order.

As mentioned previously, these "cluster problems" are simpler than avalanche distributions, but provide a powerful analytical basis for the study of transport and avalanches. Although percolation clusters are static and avalanches are dynamic, the treatment of the percolation cluster is a good way to begin to approach a process like avalanching. These clusters are somewhat analagous to drift waves with large-scale modes in that they can interact with each other, meaning that percolation clusters are good models for any system

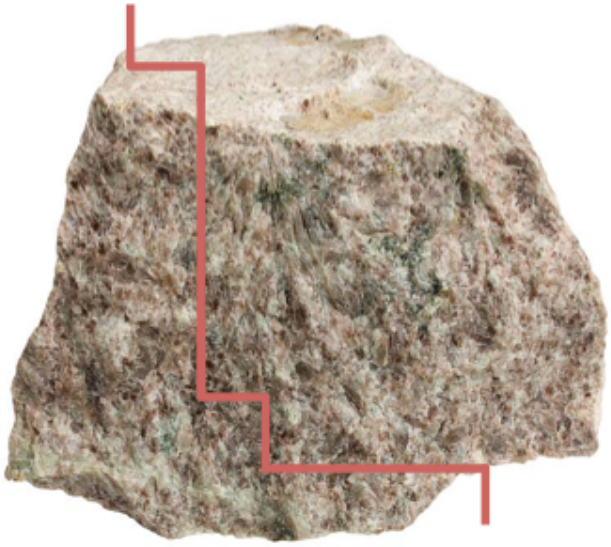

(a) A likely candidate for a holiday present to a deserving student from Patrick Diamond. Net flow of a fluid traveling through a rock experiencing a pressure gradient.

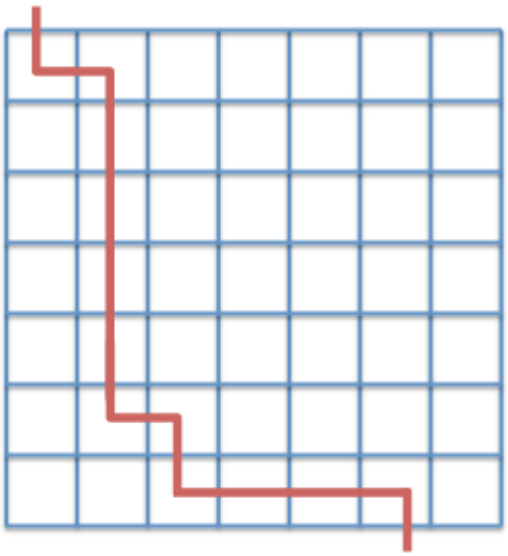

(b) Visualization of figure 3a as a random maze of pipe through which fluid can travel.

Figure 3: Net flow of a fluid travelling through a solid rock experiencing a pressure gradient, shown in two interpretations.

with short-range interactions (and avalanches happen to be of interest to plasma physics, so we study those). It also provides a relevant scientific factoid; self-organized critically was originally defined in terms of the "percolation cluster" of a single toppling [3].

2.3 "How Do I Know It When I See It?"

Now that we have established a basis for the importance of the study of percolation clusters, we can search for characteristics on how to identify these phenomena, both physically and in simulations. In and of itself, percolation is an intrinsically static concept, like a snapshot of the system in a single instant. This makes visualizing a clustering distribution as an image a useful analytical tool for our approach. Although it might appear to be your field of vision during a particularly debaucherous weekend, in figure 4, vortices cluster in 2D turbulence according to the sign of the vorticity, which are connected as different regions. This is coherent with what we would expect to see from percolation clusters, where many particles would cluster in space. (And, in the best interest of his students, Patrick Diamond has selflessly offered to give more homework assignments to any student who might be struggling with having too much free time to help forgo any temptation to engage in the nefarious activities that might result in a vortex-like headspace.)

We can introduce a time-dependence by expanding our view of percolation as a "snapshot". Time-dependence would be given as a sequence of cluster images, like a flipbook or slideshow of percolation snapshots. With transport, this sequence of images would look like an avalanche: large clusters of disturbances discharging across the system.

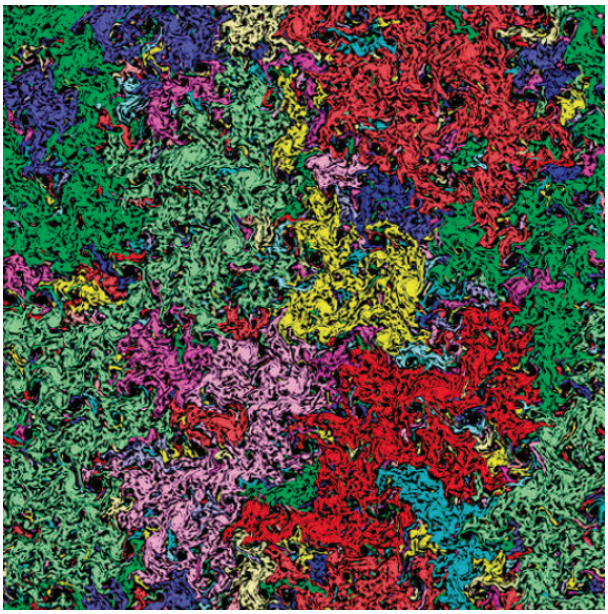

Figure 4: Vorticity clusters. These are defined as connected regions with the same sign of vorticity (here positive). Colours are arbitrarily attributed to different clusters. Regions of negative vorticity are black. L_f [the forcing scale length] is one hundredth of the box side. Taken from [4].

3 Percolation

Percolation allows us to examine prototypical, analyzable simple problems that more complex problems can be mapped to. To do this, we will develop a simple model and use tools from scaling theory.

3.1 Universality

As mentioned before, percolation is largely dependent on clusters, rather than individual elements which compose the cluster, and the shape and size of the grid on which the cluster exists. In percolation, there is no dependence on the structure and form of the elementary objects forming the percolating cluster. This is only true when the size of the percolating cluster itself is significantly larger than the elements of which it is composed. Such a condition is called universality, which is a key element of the description of percolation [5]. Because universality applies in these systems, we can apply scaling theory to examine percolation problems, which allows us to define systems as simple problems.

3.2 Where Do We Start?

We have stressed the importance of percolation to our studies and outlined the tools we need to properly examine this subject, so we can now develop our models to describe percolative behavior. To study percolation only, we begin by ignoring both D_o and ρ_e and reconsidering our topographical idea of hills and lakes. For situations with long coherence length, we have a static, random function. In diffusion, orbit dynamics play the major role in transport. In percolation, the randomness is in the system itself, and it is fixed.

Figure 5: Connected nearest neighbors (blue) isolated by empty cells (red).

As mentioned before, we will describe percolation in terms of probability distributions. In this treatment, we will think of our system as a lattice, with random occupation in all cells; that is, a probability p that a cell is occupied, and a probability $1-p$ if a cell is empty. We will refer to many elements which are connected to their nearest neighbors as "clusters", where the cluster is defined when there are connected regions of identical cells with empty sites at the end, as in figure 5.

There is some percolation threshold p_c, which is a sharply-defined critical point in a large lattice where an infinite network will permeate the lattice with a finite probability, which gives the effective length of the largest scale increase. The threshold reflects a phase transition with the condition that for p above p_c, a single percolating network will exist, and for p below p_c, no percolating network exists.

3.3 Scaling Theory for Percolation

We introduce the population density $n_s(p)$ to act as the distribution function, which is the average number per site of s clusters as a function of the probability of occupation. From this, we will take moments for the population

$$\sum_s n_s(p), \tag{3}$$

and the probability of a cluster

$$\sum_s s n_s(p), \tag{4}$$

where

$$w_s = \frac{n_s s}{\sum_s s n_s(p)} \tag{5}$$

is the probability that a cluster, to which an arbitrary site belongs, contains s sites.

We will define the percolation probability p_∞, which is the fraction of sites belonging to a percolation network, and corresponds to the "strength" of the infinite network. This allows is to relate different quantities, in the sense that any lattice site will be empty (probability of $1-p$), part of a percolation cluster (probability of $p(p_\infty)$, or part of a finite cluster (probability of $p(1-p_\infty) = \sum_s s n_s(p)$). This means that

$$1 = (1-p) + p_\infty + \sum_s s n_s(p), \tag{6}$$

which means that computing n_s will allow for the calculation of p_∞.

3.4 1D Percolation

We will examine percolation in one-dimension as a trivial, but informative case study. It is important to note that technically, percolation is not possible in only one dimension; since a single break (which is necessary to form a percolation cluster) will disconnect the "circuit" in the system, the system would break down as

defined in our context [5]. However, it is useful to consider this case to get a grasp for the treatment of probability and distribution in this analysis.

Figure 6: A five-node percolation cluster, where the blue lines represent occupied nodes and the red X's represent empty nodes.

Say we have a percolation cluster, as in figure 6, with a cluster of five surrounded by an empty node on each side of the cluster. We want to know the probability of such a structure to form. A naive assumption might be to suggest that the probability of a 5-element cluster is

$$n_s(p) = p^5, \tag{7}$$

which is incorrect because it only takes into account for the blue sticks and not the red lines. The correct assumption is to say that the probability is

$$n_s(p) = p^5(1-p)^2, \tag{8}$$

which takes into account for the 5 blue sticks and the corresponding set of 2 red X's.

Without loss of generality,

$$n_s(p) = p^s(1-p)^2, \tag{9}$$

is the thermodynamic limit in one-dimensional percolation, as $L \to \infty$ and $N \to \infty$. From this, we can see that as $s \to \infty$, $n_s(p) \to 0$, which follows a e^{-s}-like dependence.

For the one-dimensional case, the probability of a site being in a cluster of size s is

$$sn_s(p). \tag{10}$$

As a "sanity check", we also note that the probability of being in any cluster is the insightful and enlightening result

$$\sum_s sn_s(p) = p. \tag{11}$$

Recalling Eq. (5), we can compute the average cluster size, where

$$\bar{s} = \sum_s sw_s = \frac{\sum_s n_s s^2}{\sum_s n_s s}, \tag{12}$$

which is why scaling of moments is of some concern. Simplifying this, using our definition of $n_s(p)$, we see that

$$\bar{s} = \frac{\sum_s (1-p)^2 p^s s^2}{\sum_s (1-p)^2 p^s s} = \frac{1+p}{1-p}. \tag{13}$$

From this, we see that if $\bar{s} \to \infty$, $p \to p_c = 1$. If $p = 1 - \delta$, then

$$\bar{s} = \frac{2}{\delta}, \tag{14}$$

which gives us a scaling relationship for the one-dimensional case.

3.5 Percolation Near Criticality

We are primarily interested in percolation near p_c, or the percolation threshold. To develop a full, scaling solution for cluster numbers, we will use scaling theory to extract general trends of $n_s(p)$ scalings by exploiting exact solutions. We posit two scaling exponents: the first, can use the generalized 1D result in Eq. (9), and the second, the scaling exponents using power laws near the percolation threshold p_c, such that

$$f(|p - p_c|) \sim |p - p_c|^x. \tag{15}$$

From these two, we aim to understand and predict the relationship between the scaling exponents so that we can determine x from a simulation or experiment and calculate all other unknown exponents based on our analysis.

Our goal is to find the relation between these exponents. In 1D, we observe the behavior as in Eq. (9). Since we are interested in large clusters, as $s \to \infty$, the solution follows e^{-cs}, which becomes complicated, as $c \sim c(p)$ (or $c \sim |p - p_c|$) and is dependent on the probability of the cluster and therefore is not constant.

We will assume that our scaling follows a power law, $n_s(p) \sim s^{-\tau} e^{-cs}$, where $c \sim |p - p_c|^{1/\sigma}$. In a more general form,

$$n_s(p) \sim \frac{1}{s^\tau} exp(-|p - p_c|^{1/\sigma} s), \tag{16}$$

noting that $-p \simeq p_c \to 1/s^\tau$. To obtain values of τ and σ, we will use scaling from observation (by using experimental data or simulations). It is important to note that σ introduces an effective cutoff for clusters, such that

$$s < s_{cutoff} \sim |p - p_c|^{-1/\sigma}. \tag{17}$$

For steady state, s_{cutoff} defines the crossover between critical and non-critical cluster sites; there will be a contribution to the cluster average from critical clusters and no contribution to the cluster average from non-critical clusters. Thus, we define σ as the **crossover exponent**.

Since this model is limited to large clusters only, we can improve it by examining the ratio

$$\nu_s = \frac{n_s(p)}{n_s(p_c)}, \tag{18}$$

meaning that $\nu(p)$ will scale as $exp(-cs)$. This gives us $n_s(p_c) \sim s^{-\tau}$, which means that right at the threshold, the result (conveniently) scales like a power law. This result is satisfyingly simple, and it is important to note that [6]

> "You might violate the Official Secrets Act if you now conclude and say loudly that this is what theoretical physicists do; make calculations if they are easy irrespective of whether the assumptions are correct or wrong."

We now wish to relate our exponents. To do this, we can perform some calculations. Now, we will treat p_∞ as p which is the fraction of sites belonging to an infinite network $\bar{s}$. For p the possibilities for all clusters are

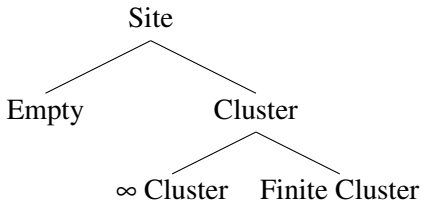

where as $s \to, n_s = 0$, which makes sense because we are looking at an infinite lattice with one network, so the total number of networks per site will be zero. We recall that the fraction of lattice sites in the infinite network is obtained from subtracting sites that belong to finite clusters from occupied sites, or

$$p + \sum_{\substack{s \\ finite}} s n_s(p) = p, \tag{19}$$

noting that $\sum_s n_s s = p_c$, since at $p = p_c$, $p = 0$. This tells us that $n_s \sim s^{-\tau}$, meaning that for convergence $\tau > 2$: a steep power law, requiring large powers for convergence. We can employ some creative accounting using Eq. (19) by employing the identity for p, explicitly writing $n_s(p)$, and plugging in p, p_c, and $s^{-\tau}$ for both. This gives us

$$p = \sum_s s^{1-\tau}(1 - e^{-cs}), \tag{20}$$

which we can convert to an integral,

$$p = \int ds \cdot s^{1-\tau}(1 - e^{-cs}). \tag{21}$$

Taking $z = cs$ and integrating by parts,

$$p = c^{\tau-2} \int dz \cdot z^{2-\tau}(e^{-z}), \tag{22}$$

which gives us the result that $p \sim c^{\tau-2}$. Previously, we anticipated that $c \sim |p - p_c|^{1/\sigma}$, meaning that

$$p = (p - p_c)^{(\tau-2)/\sigma} \tag{23a}$$
$$= (p - p_c)^{\beta}. \tag{23b}$$

Now, we have a scaling relationship between exponents, where

$$\beta = \frac{\tau - 2}{\sigma}. \tag{24}$$

Now that we have a result from scaling, we can look at how the mean cluster size diverges. For this system,

$$\bar{s} = \frac{\sum_s s^2 n_s}{\sum_s s n_s}. \tag{25}$$

As $p \to p_c$, we note that $\sum_s n_s s = p_c$. Thus,

$$\begin{aligned}
\bar{s} &= \sum_s \frac{s^2 n_s}{p_c} \\
&\sim \int ds \cdot s^2 n_s \\
&\sim \int ds \cdot s^{2-\tau} e^{-cs}, z = cs \\
&\sim c^{3-\tau} \int dz \cdot s^{2-\tau} e^{-z}.
\end{aligned}$$

This result is finite; we are neglecting the infinite single cluster. Continuing,

$$\begin{aligned}
\bar{s} &\sim c^{\tau-3} \\
&\sim |p - p_c|^{(\tau-3)/\sigma} \\
&\sim |p - p_c|^{\gamma}
\end{aligned}$$

$$\gamma = \frac{3-\tau}{\sigma}. \tag{26}$$

For $\beta > 0, \tau > 0, 2 < \tau < 3$, where β and γ are defined in Eq. (24) and Eq. (26), respectively.

We now have another way to relate our two power-law exponent. Seeing this result, however, *The Cynic* might suggest: *Do we have a new exponent for every quantity?* Unfortunately for me, since I love typing out algebra, and unfortunate for you, since you love reading algebra, the answer is **NO**! We set out/posited to obtain our two free, undetermined exponents σ (our $|p - p_c|$ behavior near criticality) and τ (our lead dependence), we have all we need to determine s_{cutoff}. We can relate all other terms to those - but first, we would need to get σ and τ from simulations or experiment.

We will consider a general case:

$$\begin{aligned}
M_k &= \sum_s s^k n_s \\
&\sim \sum_s s^{k-\tau} e^{-cs} \\
&\sim \int ds \cdot s^{k-\tau} e^{-cs} \\
& c^{\tau-1-k} \int dz \cdot z^{(k-\tau)/\sigma},
\end{aligned}$$

meaning that

$$\begin{aligned} M_k &\sim c^{\tau-1-k} \\ &\sim |p-p_c|^{(\tau-1-k)/\sigma}, \end{aligned}$$

so the scaling exponent is $(\tau-1-k)/\sigma$. This case is not rigorous - there are "glitches" where the model falls apart - but it captures the essence of scaling and how we are successful using this approach.

We can look at the more general derivation - but first, making a quick caveat to acknowledge that [6]

> "If you have read this far through the book, it is presumably too late for you to return it for a refund."

The author extends her appreciation for your interest in the mathematics behind percolation, and hopes you enjoy the general derivation as much as the previous results.

The general derivation is the stretched out, exponential version of the previous result from Eq. (16).

$$n_s(p) \sim \frac{1}{s^\tau} f((p-p_c)s^\sigma), \tag{27}$$

where p_c and $s \gg 1$ and we have replaced the exponential function seen previously with some function that can be determined from computation. This will behave well in all cases, which we can check with our previous results,

$$\begin{aligned} \bar{s} &= \sum_s s^2 n_s \\ &\sim |p-p_c|^{(\tau-3)/\sigma} \\ &\sim |p-p_c|^{-(3-\tau)/\sigma} = |p-p_c|^\gamma, \end{aligned}$$

where γ is the same as the exponent defined in Eq. (26) which we saw before. Thus, the exponents γ and β are universal, and have an independent lattice structure (see Section 3.5). Higher dimensions will lead to fractal perimiters on clusters (and they usually are). We can also extend the fun of this exercise to correlation lengths, perimeters in two dimensions, and other exciting fields.

Table 1: Scaling relationships for a 2D lattice. All of these cases are valid only for $p \to p_c$. The 1D case is included, though its scaling relationship is not exponential.

Quantity	Cluster Equation	Probability	Exponent	Scaling Exponent	Scaling Relationship
Population	$\sum_s n_s(p)$	$\lvert p-p_c\rvert^{2-\frac{\tau-1}{\sigma}}$	$2-\frac{\tau-1}{\sigma}$	α	$\lvert p-p_c\rvert^{(2-\alpha)}$
Probability of a Cluster	$\sum_s s n_s(p)$	$\lvert p-p_c\rvert^{\frac{\tau-2}{\sigma}}$	$\frac{\tau-2}{\sigma}$	β	$\lvert p-p_c\rvert^{(\beta)}$
Mean Cluster Size	$\sum_s s^2 n_s(p)$	$\lvert p-p_c\rvert^{\frac{3-\tau}{\sigma}}$	$\frac{3-\tau}{\sigma}$	γ	$\lvert p-p_c\rvert^{(-\gamma)}$
Correlation Length	$\xi(p)$	$\lvert p-p_c\rvert^{\frac{n_s(p)}{n_s(p_c)}}$	$\frac{n_s(p)}{n_s(p_c)}$	ν	$\lvert p-p_c\rvert^{(-\nu)}$
Average Cluster Size (1D)	$\sum_s s w_s$	$\frac{1+p}{1-p}$	$p-1$	δ	$\frac{2}{\delta}$

3.6 Classic Percolation Problem

One of the classic percolation problems (discussed in [5] and [7], among others) is the study of the effective conductivity of random mixture. This problem has wide applicability to the calculation of conductivity in inhomogeneous films, surface conductivity in unevenly covered surfaces, and magnetized plasmas with instabilities in the plane perpendicular to the magnetic field. We see that the conductivity in a two-phase system is the geometric mean of the conductivity of both phases. To examine this problem, we assume a medium consisting of two species (of arbitrary shapes and dimensions) where the scale of the overall system is significantly larger than the scale of its elements, which sounds familiar to the conditions for a system which can undergo percolation.

The solution to this problem begins with Ohm's law, $\mathbf{j} = \sigma\mathbf{e}$, where σ is the conductivity, and the equations of constant current, or $rot\mathbf{e} = 0$ and $\nabla \cdot \mathbf{j} = 0$. For this case, we will assume the conductivity is a random function of (x,y). Further, the system has two regions (1 and 2) which are statistically equivalent, each with a conductivity $\sigma = \sigma_1, 2$. We are looking for the relationship between the current (averaged over the system) and the average field, or

$$\mathbf{J} = \frac{1}{V}\int dV \cdot \mathbf{j} \tag{28a}$$

$$\mathbf{E} = \frac{1}{V}\int dV \cdot \mathbf{e}, \tag{28b}$$

respectively. The linearity of Ohm's law and the equations of constant current mean that Eq. (28) will also be linear, which means the system is isotropic as a whole and can be represented by a simple scalar relationship,

$$\mathbf{j} = \sigma_{eff}\mathbf{E}, \tag{29}$$

where σ_{eff} is the effective conductivity of the medium. Since the medium is uniform for this case, we can assume σ_{eff} is an averaged macroscopic quantity which will disperse with an increase in volume. Thus, we will introduce new unknowns to satisfy this quality, such that

$$\mathbf{j'} = (\sigma_1\sigma_2)^{1/2}(\mathbf{n}\times\mathbf{e}) \tag{30a}$$
$$\mathbf{e'} = (\sigma_1\sigma_2)^{-1/2}(\mathbf{n}\times\mathbf{j}), \tag{30b}$$

where $\mathbf{n}$ is the unit normal to the xy-plane. Putting in our new unknowns into Ohm's law and the equations of constant current, we have a new system of equations, such that

$$\mathbf{j'} = \sigma'\mathbf{e}' \tag{31a}$$
$$\sigma' = \sigma_1\sigma_2/\sigma \tag{31b}$$
$$rot\ \mathbf{e}' = 0 \tag{31c}$$
$$\nabla\cdot\mathbf{j}' = 0. \tag{31d}$$

We now have a new conductivity σ'. Since our regions 1 and 2 are statistically equivalent, this corresponds to an averaged Ohm's law of

$$\mathbf{J}' = \sigma_{eff}\mathbf{E}', \tag{32}$$

where σ_{eff} is the same as in Eq. (29). From Eq. (30), we see that

$$\mathbf{J'} = (\sigma_1\sigma_2)^{1/2}(\mathbf{n}\times\mathbf{E}) \tag{33a}$$
$$\mathbf{E'} = (\sigma_1\sigma_2)^{-1/2}(\mathbf{n}\times\mathbf{J}), \tag{33b}$$

and we can combine Eq. (32) with Eq. (33) to see that

$$\sigma_{eff} = (\sigma_1\sigma_2)^{1/2}, \tag{34}$$

meaning that the logarithm of the conductivity is additive upon mixing. This expression will be true for systems of equal random media, like our percolation problems, and would apply to the board of tiles discussed in Section 1.

This can also be expanded to include less rigorous restrictions on the form of the function $\sigma(x,y)$. We will introduce the quantity $\chi(x,y) = \ln\sigma - \langle\ln\sigma\rangle$ so that we can consider an ensemble of systems where the multi-point conductivity distribution function is an even function of χ. We will assume a Gaussian distribution for χ and make the substitution

$$\mathbf{j'} = \exp(\langle\ln\sigma\rangle)(\mathbf{n}\times\mathbf{e}) \tag{35a}$$
$$\mathbf{e'} = \exp(-\langle\ln\sigma\rangle)(\mathbf{n}\times\mathbf{j}), \tag{35b}$$

meaning Ohm's Law transform from $j = (\exp(\langle \ln \sigma \rangle + \chi)\ \mathbf{e})$ to $j' = (\exp(\langle \ln \sigma \rangle - \chi)\ \mathbf{e'})$.

Here, we replaced χ with $-\chi$ and used the fact that the distribution function is even in χ, we see that the new, prime system is macroscopically equivalent to the original. Following the same treatment discussed in the previous case, we see that

$$\sigma_{eff} = \exp \langle \ln \sigma \rangle = (\langle \sigma \rangle / \langle 1/\sigma \rangle)^{1/2}. \tag{36}$$

For the Gaussian distribution, this will take the form

$$\sigma_{eff} = \langle \sigma \rangle \exp(-\Delta^2/2),$$

where $\Delta = \langle \chi^2 \rangle^{1/2}$ is the root mean square fluctuation of the natural logaritm of the conductivity.

3.7 Percolation in Magnetic Fields

Now that we have a basic understanding and grasp of percolation, we will bring our discussion back to the field of plasma physics to examine percolation in magnetic fields. This phenomenon is important to consider because it affects charged particles moving along lines, which can change the global plasma parameters (such as conductivity in fusion plasmas). Tangling of magnetic lines can also determine diffusive and heat conductive processes.

Percolation in magnetic fields occurs in regimes with large Kubo number ($Ku \gg 1$). We will study only the extreme cases, with the understanding that the actual physical picture will be represented somewhere in between these situations. For cases of 2D static random media where $l_{ac} \to \infty$ and $\tau_{ac} \to \infty$ (as previously mentioned, this is one end of the extreme, since l_{ac} is finite in reality). We will the two-dimensional magnetic field b as

$$b_x = \frac{\partial A}{\partial y} \tag{37a}$$

$$b_y = -\frac{\partial A}{\partial x}, \tag{37b}$$

where we will assume that the vector potential $\mathbf{A} =< 0, 0, A >$ is independent of t and z, meaning that we can treat the problem as a random function of two variables x and y. We use a spectral representation, where the Fourier transform of A will give the field configuration, or the spatial structure of the actual system, as

$$\langle A_k^2 \rangle \simeq e^{-k^2/k_0^2} \tag{38}$$

when $k \gg k_0$. For large scales (where $n > 0$ and $k \ll k_0$),

$$\langle A_k^2 \rangle \simeq \left(\frac{k}{k_0}\right)^{2n}. \tag{39}$$

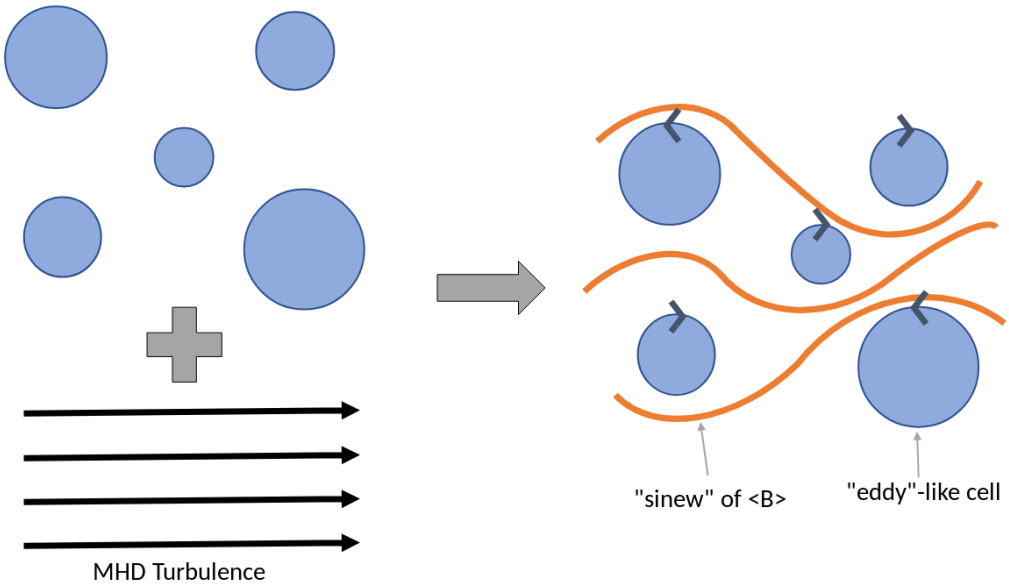

Figure 7: Percolation of magnetic field lines in $Ku > 1$.

To have some notion of the spectrum of A, the distribution of $\langle A_k^2 \rangle$ will still have the same features we would expect to see, with hills and lakes and critical scalings. In other words, we have a small auto-correlation at large distance.

In 2D, for $Ku > 1$ systems, $\langle B \rangle \neq 0$ and $\tilde{B} \gg \langle B \rangle$, meaning that the fluctuations are greater than the mean field. This is the case in the solar tachocline or the weather layer of Jupiter, where there is a surface layer that is spatially stratified between convective and radiative layers.

If we want to know what the field actually looks like, we can imagine an ensemble of cells, illustrated in figure 7, where $\nabla \cdot \mathbf{B} = 0$. When these cells experience MHD turbulence, patterns emerge; the system looks like flow with eddies, where the cells move in a circle like a vortex as the field "flows" past. In this scheme, the field moves like "sinews" of $\langle B \rangle$ through the network of eddy-like cells.

Since we are looking at extreme cases, we may wonder: does the large-scale $\langle B \rangle$ percolate as the system size a approach infinity? What *would* happen to the mean field if we *actually* had an infinite system? When will the mean extend, or percolate?

To investigate this, we connect the spectrum of A to real space structure. We will say that $A_k \sim k^m$ and $B_k \sim k^{m+1}$, and from this, noting that

$$\langle B \quad \rangle \sim \left(\langle b^2 \rangle_{k<1/a} \right)^{1/a} \tag{40a}$$

$$\sim \int_0^{1/a} dk \cdot k k^{2m} k^2 \tag{40b}$$

$$\simeq \left(\frac{1}{a}\right)^{-m-2}. \tag{40c}$$

Thus, $\langle B \rangle$ is finite as $a \to \infty$ where $m = -2$. Now, we must consider what must happen with the current for this case to hold. Since $j_{z,k} \cong k^2 A_k \sim k^0$ is constant, there must be a white noise current spectrum if

there is a percolating magnetic field. For this case, $\langle \hat{j}^2 \rangle$ is approximately constant. We see that $\langle j(\bar{x}) j(\bar{x} + \bar{r}) \rangle > 0$, which are correlated currents (noting that anti-correlated currents will fail, as the fields they create will cancel). This is the importance of the large-scale spectrum, where the Loitsyansky integral indicates large-scale turbulence. We must have non-screened, non-compensated currents in order to see magnetic percolation in a system.

4 Classical Problems in High Kubo Transport

Recalling our discussion of transport in a 2D stochastic magnetic field, we remember that particles could be "kicked off" a line via diffusive processes. Now, we can apply this discussion of percolation to examine the case where cells are close, and collisional diffusion can kick particles from one cell to another, rather than kicked off of a field line, shown in figure 8. Such cases describe the interaction of collisional transport with fixed laminar flow and no time dependence. Here, the autocorrelation time $\tau_{ac} \to \infty$ and $Ku \gg 1$, which fixes the systems into effectively static patterns that we can analyze. In simple terms, flow, collisions, and diffusion interact, which results in transport. It is important to note that these cases are particularly significant because the slow diffusive processes introduce irreversibility into these schemes.

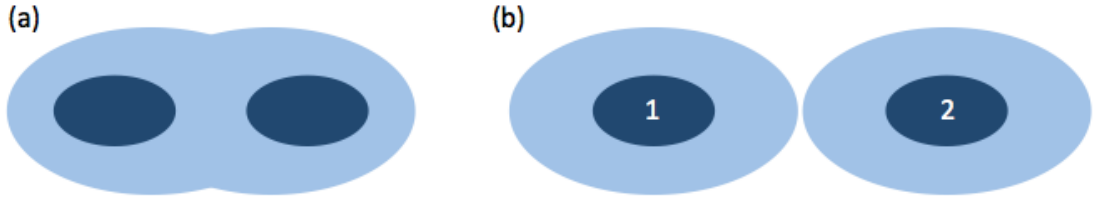

Figure 8: The theme of our previous discussions was diffusive "kicks" off of field lines, akin to a system shown in (a). Collisional diffusion, discussed here, can "kick" a particle from (1) to (2) in (b), if cells are close.

Many problems involve the synergy between turbulent scattering and collisional diffusion. Here, two such toy problems are presented, courtesy of G. I. Taylor (see Appendix A), both of which show the interaction between static cells (as in Section 4.1) or shear (as in Section 4.2) and diffusion and the dependence of such problems on the actual geometry of the system.

4.1 Taylor Cell Problem

The Taylor Cell Problem allows for the calculation of effective diffusivity within a system with both fast and slow diffusive processes. It involves a system of individual convection cells situated within a concentration gradient (see figure 9).

The system has a background diffusivity D_0 driven by the concentration gradient (see figure 10) and a cell diffusivity of D_{cell} introduced by convection.

Our goal with this problem is to find out the effective diffusivity in the system; that is, we are seeking D_{eff} in

$$\langle \Gamma_c \rangle = -D_{eff} \nabla \langle C \rangle, \tag{41}$$

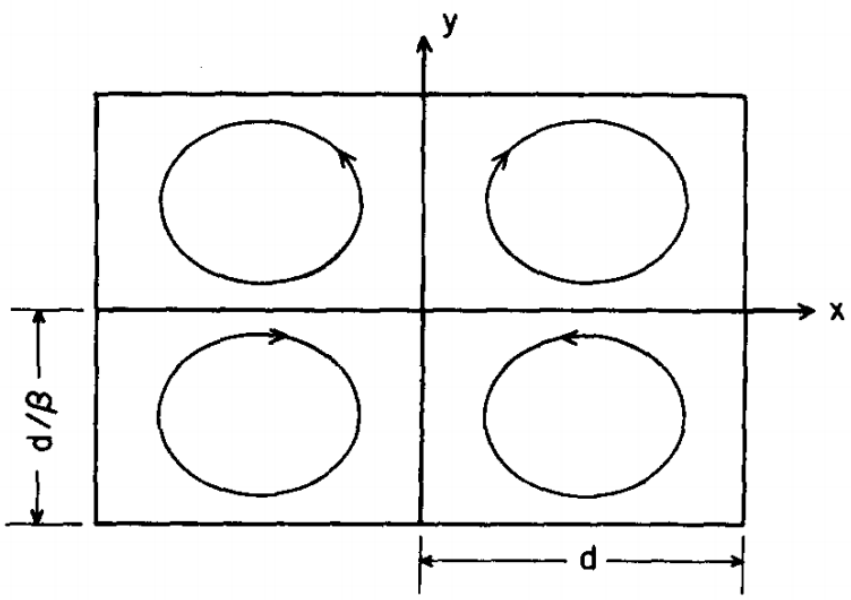

Figure 9: Circulation pattern for rolls with a periodicity $2d$ in the x direction and $2d/\beta$ in the y direction. Taken from [8].

where the scale of the brackets $\langle\cdot\rangle$ denotes the average across the entire system (that is, the dashed line in figure 10, rather than the localized "steps" in the stair configuration).

We assume the system is isotropic, and that there is diffusion (which is necessary to get from one cell to another - if there is no convection, the particle will be trapped in a single cell). Let v_0 be the circulation speed in each cell, l_0 be the circulation length, and δ_0 be the boundary layer thickness, set by diffusion, such that

$$\delta^2 \sim D_0 \frac{l_0}{v_0}, \tag{42}$$

where l_0/v_0 is the transit time through the boundary layer.

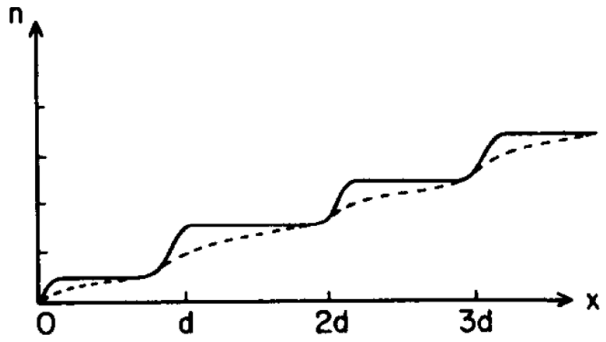

Figure 10: Schematic density profile for dye along the x direction. Steep transition in the density exist between each cell. Taken from [8].

For a heuristic argument of D_{eff}, we can use the relationship

$$D_{eff} \sim f_a \frac{(\Delta x)^2}{\Delta t}, \tag{43}$$

where $\Delta x \sim l_0$ and $\Delta t \sim l_0/v_0$. Since all diffusion happens in a space proportional to the boundary layer thickness between cells, we introduce $f_a = \frac{\delta}{l_0}$, which is the volume fraction of the space where the diffusion in the system occurs. For this system, Eq. (43) can be written as

$$D_{eff} \sim \frac{\left(\frac{D_0 l_0}{v_0}\right)^{1/2}}{l_0} \frac{l_0^2}{\frac{l_0}{v_0}}, \tag{44}$$

meaning that

$$D_{eff} \cong (D_{cell} D_0)^{1/2} = D_o Pe^{1/2} \tag{45}$$

where $Pe = \frac{v_0 l_0}{D_0}$ is the Péclet number, or the ratio of advective to diffusive transport in problems dealing with concentration.

It is important to emphasize that this is the result for net transport; it is **NOT** a simple addition - $D_{eff} \neq D_0 + D_{cell}$!

4.2 Taylor Shear Dispersion Problem

The Taylor Shear Dispersion Problem deals with dispersion in a laminar flow and shows the effect of velocity shear on the diffusion of dye in a pipe or channel. We examine three cases, illustrated in figure 11. The first case is the "base case": diffusion of a dye with no flow. The second case is flow in a pipe with an artificial "slip" boundary condition, where velocity at the walls is nonzero. The third case represents physical laminar flow through a pipe (with the no-slip boundary condition at the walls).

In figure 11(a), we expect the diffusion coefficient to be proportional to the expansion rate of the dye, or

$$\delta r \sim \sqrt{D_o t},$$

which is a time-asymptotic argument where $t \gg L_\perp^2/D_0$.

In figure 11(b), we expect the diffusion coefficient to be proportional to the expansion rate of the dye as it travels along the tube, or

$$\delta l \sim \sqrt{D_o t}.$$

In this case, since there is no shear introduced at the boundary, the diffusion across the pipe or channel is faster than the diffusion along the pipe. As such, the dispersion will occur in the lateral direction, but move down the pipe as one unit.

In figure 11(c), the system will eventually reach a stage where the shear at the wall will "pull" the dye back as it moves along the channel, making the concentration front appear relatively flat. For this case, we expect a similar scaling relation as the previous case, but using the effective diffusion coefficent instead of the ambient,

$$\delta l \sim \sqrt{D_{eff} t},$$

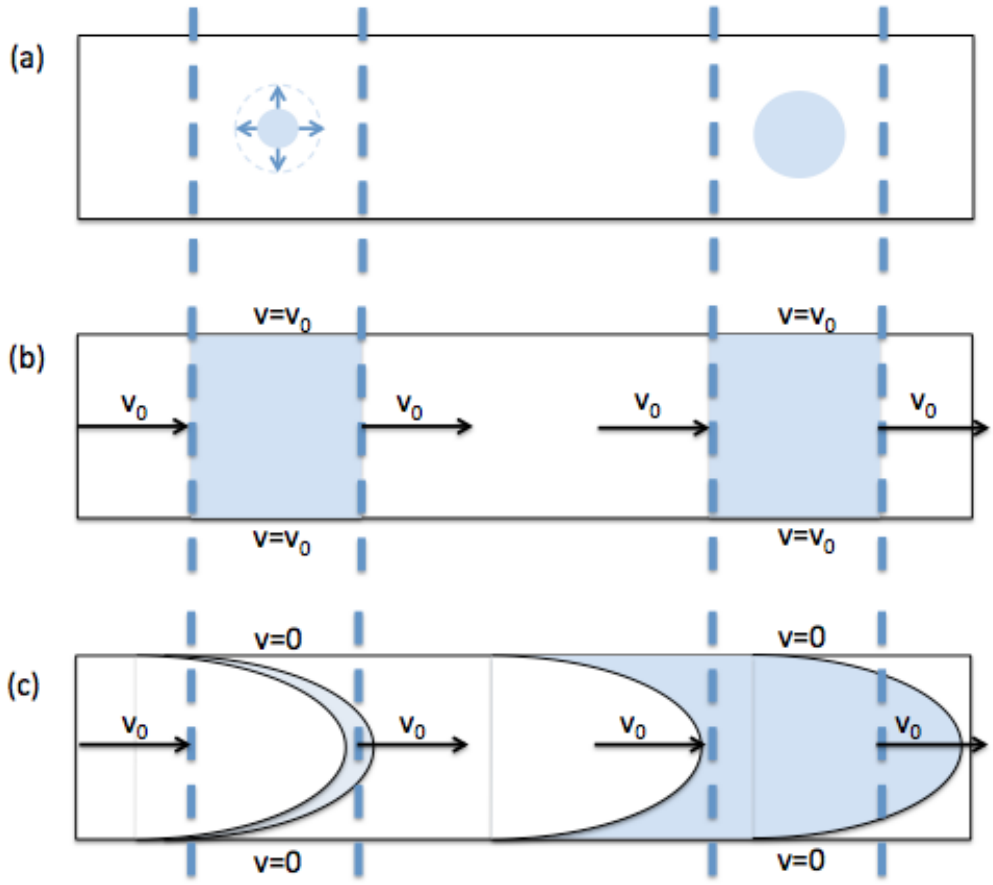

Figure 11: Dispersion profile of concentration in laminar flow for no flow (Figure (a)), an artificial "slip" boundary condition with nonzero velocity at the boundary, (Figure (b)), and the traditional "no-slip" boundary condition (Figure (c)).

since $D_{eff} \gg D_0$ because of the shear dispersion from the boundary condition. For this case, the key observation is that shear flow will lead to stretching and spreading in the fluid, while diffusion will provide orthogonal spreading. As such, we expect that the diffusion in this system will be the simple addition of the ambient diffusion and shear, or $D_{eff} = D_0 + D_{shear}$.

To calculate D_{shear} for the third case, we start with the full transport equation in terms of concentration, or

$$\frac{\partial c}{\partial t} + v \cdot \nabla c = D_0 \nabla^2 c, \tag{46}$$

where $v(y,z) = 2\frac{u}{a^2}(a^2 - y^2 - z^2)$. We introduce a time-scale separation, such that

$$\langle c \rangle = \frac{1}{a} \int_{-a/2}^{a/2} dy \cdot c(x,y,t) \tag{47a}$$

$$\langle v \rangle = \frac{1}{a} \int_{-a/2}^{a/2} dy \cdot v(x,y,t), \tag{47b}$$

and "twiddles", or fluctuations from the mean,

$$\tilde{c} = c - \langle c \rangle \tag{48a}$$
$$\tilde{v} = v - \langle v \rangle, \tag{48b}$$

where $\tilde{v}$ is the deviation from the exact flow of the channel average. Looking at the full transport equation for our twiddles in Eq. (48), we see that

$$\frac{\partial \langle c \rangle}{\partial t} + \langle v \rangle \frac{\partial \langle c \rangle}{\partial x} + \frac{\partial \langle \tilde{c}\tilde{v} \rangle}{\partial x} = D_0 \frac{\partial^2 \langle c \rangle}{\partial x}, \tag{49}$$

where $\langle \tilde{v}\tilde{c} \rangle = -D_{shear} \frac{\partial \langle c \rangle}{\partial x}$. We now subtract Section 4.2 from Eq. (46), yielding a final result of

$$\left[\frac{d}{dt}\tilde{c}\right] = \frac{\partial \tilde{c}}{\partial t} + \langle v \rangle \cdot \nabla \tilde{c} - D_0 \nabla^2 c \tag{50}$$

for the averaged equation. The exact equation gives us

$$\left[\frac{d}{dt}\tilde{c}\right] = -\tilde{v}\frac{\partial \langle c \rangle}{\partial x} + D_0 \frac{\partial^2 \tilde{c}}{\partial y^2}, \tag{51}$$

where the first term corresponds to the stretching of the flow beyond the mean (from shear) and the second terms corresponds to perpendicular diffusion that works against stretching. Since there is no turbulence here, the only dissipation in the system occurs via shear laminar flow and diffusion.

Now, we must take into account that the pipe has a finite orthogonal length scale, which allows us to define a natural time scale for the system - which is in the frame, co-moving with the mean flow - of $\tau_{\perp,diff} \sim L_\perp^2 / D_0$. For $t \gg \tau_{diff}$, the system is diffusively damped, meaning that at steady state,

$$\tilde{v}\frac{\partial \langle c \rangle}{\partial x} = D_0 \frac{\partial^2 \tilde{c}}{\partial y^2}. \tag{52}$$

Reintroducing our beloved twiddles (from Eq. (48)), we can allow for a scale difference by Fourier expanding to

$$\tilde{c} = \sum_{k_y} e^{iky} \langle \tilde{c}_{k_y} \rangle \tag{53a}$$
$$\tilde{v} = \sum_{k_y} e^{iky} \langle \tilde{v}_{k_y} \rangle, \tag{53b}$$

noting that $k_{y,min} \cong 2\pi/L_\perp$. Therefore,

$$\tilde{c}_{k_y} = \frac{-1}{k_y^2 D_0} \tilde{v}_{x,k_y} \frac{\partial \langle c \rangle}{\partial x}$$
$$\tilde{v}_{x,k_y} \frac{\partial \langle c \rangle}{\partial x} = -k_y^2 D_0 \tilde{c}_{k_y}.$$

We are looking for

$$\langle \tilde{v}_x \tilde{c} \rangle = \sum_{k_y} \frac{-|\tilde{v}_{x,k_y}|^2}{k_y^2 D_0} \frac{\partial \langle c \rangle}{\partial x},$$

and recalling

$$\frac{\partial \langle c \rangle}{\partial t} + \frac{\partial \langle \tilde{c}\tilde{v} \rangle}{\partial x} = D_0 \frac{\partial^2 \langle c \rangle}{\partial x},$$

we can conclude that since $D_{eff} = D_0 + D_{shear}$,

$$D_{shear} = \sum_{k_y} \frac{|\tilde{v}_{k_y}|^2}{k_y^2 D_0}, \tag{55}$$

or

$$D_{shear} = c \frac{v_0^2 L_\perp^2}{D_0}, \tag{56}$$

where c is some form factor. This means that the effective diffusion for this laminar, shear-flow case is

$$D_{eff} = D_0 + c \frac{v_0^2 L_\perp^2}{D_0}. \tag{57}$$

It is important to note that for laminar flow, it is possible for $D_{shear} \gg D_0$. in which case we would see enhanced along stream (or in frame) diffusivity and enhanced shear dispersion.

4.3 Limitations

While these cases are informative, it is important to note their shortcomings. These are both asymptotic results: they are only valid for $t \gg L_\perp^2/D_0$. The models are only valid for laminar, unidirectional flow - for example, we would not be able to apply these models for bidirectional shear flow with flow reversal, as few of our assumptions would still apply.

5 Conclusions and Final Remarks

The general message of large Kubo number transport allows us to form a basis for more complicated phenomena. It is important to remember that large-scale emergent behavior occurs in systems with local interaction. Systems can self-organize in a hierchy of clusters, that diverge at criticality, where criticality can be reached by a perturbation in some respect to the system. Our analysis was made possible by percolation having the property of universality, which meant that we could use scaling and then power laws to build our model. Scaling theory is a powerful and useful phenomenology which links scaling exponents, which means our models can be expanded for more complex systems. It is imperative to recall that the answer is **always** an exponent!

The overall punchline with this summary, and the main takeaway that I hope sticks with you forever and ever, is that emergent critical behavior as $l_c \to \infty$ indicates that transport phenomena exist that are **not** captured by random walk models. We investigated $Ku \gg 1$ schemes, but it is important to remember the complication of emergent critical behavior and the breakdown of the diffusive model in any aspect of your life!

Appendices

A On Finding a Good Tailor: A Guide

To conclude our discussion on percolative transport, I present a short caveat to provide a brief (albeit painfully incomplete) guide to the multitude of Taylors found in the annals of plasma physics, fluid mechanics, and other turbulent processes.

A.1 G.I. Taylor

Sir Geoffrey Ingram Taylor, O.M. F.R.S. H.F.R.S.E. (7 March 1886 – 27 June 1975) was a prolific physicist whose work in fluid dynamics and wave theory had a profound impact on science and engineering in the 20th century. Throughout his career, he researched light wave propogation, shock waves, atmospheric mixing, turbulence, aircraft design, mechanical stress, oceanography, rotational fluids, crystalline and plastic deformation, solid mechanics, the Manhattan Project, gas physics, boat design [9], and many other topics pertaining to transport and static materials [10].

A.2 J.B. Taylor

John Bryan Taylor, F.R.S. (14 January 1929 -) is a plasma physicist and fellow of the Royal Society [11]. His research involved seminal work on bootstrap current, ballooning theory, scaling theory, and gyrokinetics, which have significant implications for future fusion research. He is still working on theoretical fusion research part-time at Culham [12].

A.3 R.J. Tayler

Roger John Tayler, F.R.S., O.B.E. (25 October 1929 - 23 January 1997) was an astronomer and physicist known for his work in astrophysics and plasma stability. While he gained notoriety primarily for his work in astrophysics, he studied magnetohydrodynamic stability, expanding upon work being conducted on kinking and fluting and proposing the addition of an axial magnetic field on a cylindrical discharge, which improves plasma stabilization by distorting unstable modes to feed energy into the axial field. Tayler's work also involved the study of the newly-proposed MHD energy principle, applying it to his cylindrical discharges and studying MHD stability. Additionally, Tayler studied the effects of MHD on convection in compressible fluids, which has implications in the field of solar astrophysics [13].

A.4 R.J. Taylor

Robert John Taylor was the principal investigator and designer of the UCLA Electric Tokamak (ET), which (at the time of its construction) was the largest device of its kind in the world [14], and, with Ron Parker, was one of the leaders of the Alcator-A machine, and one of the co-discoverers of Alcator scaling. Taylor is also the inventor of discharge cleaning, and did key experiments on bias-driven H-mode on CCT. Of particular relevance to the UC San Diego community, he was also the Ph.D. advisor to our own Associate Dean of Engineering, Professor George Tynan [15]. Taylor is currently retired.

References

(1) Broadbent, S.; Hammersley, J. M. Percolation processes. *Mathematical Proceedings of the Cambridge Philosophical Society* **1957**, *53*, 629–641.

(2) Larson, G., *The Far Side*.

(3) Bak, P.; Tang, C.; Wiesenfeld, K. Self-Organized Criticality: An Explanation of 1/f Noise. *Physical Review Letters* **1987**, *59*, 381–384.

(4) Bernard, D. et al. Conformal invariance in two-dimensional turbulence. *Nature Physics* **2006**, *2*, 124–128.

(5) Zeldovich, Y. B.; Sokoloff, D. D.; Ruzmaikin, A. A., *The Almighty Chance*, 1990, pp 141–163.

(6) Stauffer, D.; Aharony, A., *Introduction to Percolation THeory*, 2nd ed.; Taylor and Francis: London, England, 1991, pp 37,42.

(7) Dykhne, A. M. Conductivity of a Two-Dimensional Two-Phase System. *Soviet Physics JETP* **1971**, *32*, 63–65.

(8) Rosenbluth, M. N. et al. Effective diffusion in laminar convective flows. *Physics of Fluids* **1987**, *30*.

(9) Taylor, S. G. I. The Holding Power of Anchors. *The Yachting Monthly and Motor Boating Magazine* **April 1935**, DOI: https://www.petersmith.net.nz/boat-anchors/docs/taylor-the-holding-power-of-anchors-1934.pdf.

(10) Batchelor, G. *Geoffrey Ingram Taylor*; Biographical Memoirs of Fellows of the Royal Society; Brighton, United Kingdom: The Royal Society, 1976.

(11) *List of Fellows of the Royal Society 1660 – 2007*; A complete listing of all Fellows and Foreign Members since the foundation of the Society; London, United Kingdom: The Royal Society Library and Information Services, 2007.

(12) Hay, J. Eighty years young., https://www.iter.org/newsline/66/199, 26 Jan. 2009.

(13) Mestel, L.; Pagel, B. *Roger John Tayler, O.B.E.* Biographical Memoirs of Fellows of the Royal Society; Brighton, United Kingdom: The Royal Society, 1998.

(14) Taylor, R. J. *UCLA Tokamak Program Close Out Report*; Technical Report DOE-UCLA53225-Final Report; Los Angeles, United States: University of California, Los Angeles, California, 2014.

(15) Diamond, P. H., personal communication, 2019.